Radiocarbon, Vol 64, Nr 5, 2022, p 969–987 DOI:10.1017/RDC.2022.58

CHRONOLOGY OF IBA SHAFT TOMBS IN THE SOUTHERN LEVANT: INTEGRAL PART OF THE IBA CULTURE FROM BEGINNING TO END

Ron Lev[1]* • Yehuda Govrin[2] • Zach Horowitz[3] • Eugenia Mintz[1] • Lior Regev[1] • Elisabetta Boaretto[1]*

[1]D-REAMS Radiocarbon Laboratory, Weizmann Institute of Science, Rehovot, Israel
[2]The Nelson Glueck School of Biblical Archaeology, Hebrew Union College, Jerusalem, Israel
[3]Israel Antiquities Authority, Jerusalem, Israel

ABSTRACT. Vast burial fields, some with hundreds of burials, categorize the southern Levant's Intermediate Bronze Age period (IBA). This phenomenon contrasts with a limited number of burials found from the preceding Early Bronze III period. This paper presents the first radiocarbon dating research of sampled bones from shaft tombs from five IBA burial sites across Israel: Yehud, Jebel Qaaqir, Sheikh-Danon, Hazorea, and Kefar-Veradim. Prescreening methods, including Fourier transform infrared analysis, were applied to identify best-preserved collagen in archaeological bones for radiocarbon dating. Overall, the measured date ranges cover the IBA timeline, supporting the observation that the IBA signature shaft tombs are a fundamental tradition of the IBA culture, at least in Israel. A single IBA shaft tomb at Jebel Qaaqir which contained remains of multiple humans, supplied different dates for various people, spanning over a few hundred years. These results suggest a tribal or family-oriented IBA community with a long-lasting tradition reflected in centuries of collective burial practices.

KEYWORDS: Intermediate Bronze Age, radiocarbon dating, southern Levant, Shaft tumbs.

INTRODUCTION

The Intermediate Bronze Age (IBA hereafter, also known as EB-IV) populated the southern Levant in the second half of the third millennium BCE. It was a pastoral-rural culture with clear differentiation in settlement patterns and material culture from the urban Early-Bronze III culture (EB-III) preceding it. Scholars identify distinct cultural aspects in IBA, including, among others, its burial habits. Dozens of IBA burial sites, some containing hundreds of tombs, have been discovered to date (Figure 1). Most IBA burials include grave goods accompanying the deceased on their eternal journey, mainly pottery vessels, copper alloy objects, beads, and animal parts. The most common IBA burials found are in shaft tombs, dug into the bedrock, or in the ground. One type is a primary burial(s) within a single chamber (Figure 2a), as in the burial fields of Bet Dagan (Yannai et al. 2014), Yehud (Govrin 2015), and some Jericho tombs (Kenyon 1965). Another shaft tomb type is of secondary burials with disarticulated bones within one or several tomb chambers (Figure 2b), as in Megiddo (Guy 1938), Hazorea (Meyerhof 1989), and Jebel Qaaqir (Dever 2014). Less common are IBA cist tombs that are stoned-lined or slab-roofed (Figure 2c), as in Tell el-Ajjul (Kennedy 2015) and Tiwal esh-Sharqi (Tubb 1990). Some dolmen and tumulus/cairn burials were also attributed to the IBA (Figure 2d), e.g., in the Golan (Epstein 1985; Sharon et al. 2017) and the Negev (Dever 2014:213–216). Major IBA burial sites were excavated, among others, also at Beth Shan (Oren 1973), Lachish (Tufnell 1958), Gibeon (Prichard 1963), 'Ein Asawir (Horowitz 2016), Dhahr Mirzbaneh (Lapp 1966), 'Ein Samiya (Dever 1972), Tiwal esh-Sharqi (Helms 1983; Tubb 1990), Umm el-Bighal (Helms et al. 1988), and Khirbat Iskandar (Richard et al. 2010).

*Corresponding authors. Email: Levronny@gmail.com, Elisabetta.Boaretto@weizmann.ac.il

Figure 1 Southern Levant map indicating IBA settlements and burial grounds. Red circles indicate burial grounds that were ^{14}C dated within this research. (Please see online version for color figures.)

https://doi.org/10.1017/RDC.2022.58 Published online by Cambridge University Press

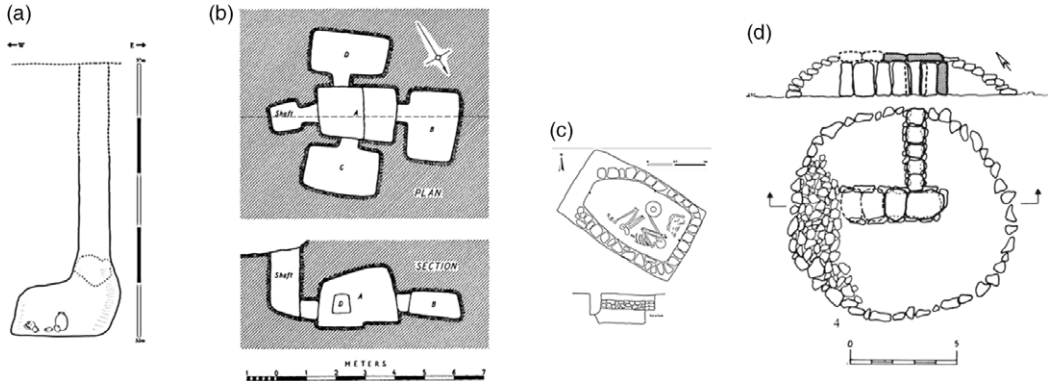

Figure 2 Examples of IBA tomb types: (a) Single chamber shaft tomb at Yehud (redrawn after Govrin 2015: Fig. 119). (b) Multiple chamber shaft tomb at Megiddo (redrawn after Guy 1938: Fig. 42). (c) Cist tomb at Tell el-Ajjul (redrawn after Kennedy 2015: Fig. 4). (d) Dolman plan from the Golan (redrawn after Epstein 1985: Fig. 1).

EB III sites with substantial burial activity are an exception. Such sites are Jericho with rock-hewn tombs and Bab edh-Dhra with unique above-the-ground charnel houses. Other than that, only several more tombs in the southern Levant were attributed to EB-III (Ilan 2002:96–99 with references). The vast number of burials discovered from the IBA is in striking contrast to the low number of tombs found from the preceding period of EB III. Yet, the published IBA absolute dates are from settlements, not burials. A possible exception is one date from a multiperiod tomb at Tell al-Husn in northern Jordan (Al-Muheisen et al. 2012).

The EB "High Chronology" based on a systematic analysis of ^{14}C dates suggests that EB III cities ceased to exist around 2500 BCE, and IBA sites already existed around the same time (Regev et al. 2012, 2014; Höflmayer et al. 2014; Lev et al. 2020; Fall et al. 2021). The high chronology extended the duration of the IBA period from about 300 years in the previous consensus (Mazar 1990; de Miroschedji 2009) up to 500 or 600 years. It is essential to determine when the drastic change in burial practices between EB III and IBA (described above) occurred within the IBA duration of half a millennium. When did IBA-type burials start? Were they common throughout all of the IBA period? Exploring this item can help us better understand the IBA culture and its development. Although progress has been made lately in IBA pottery relative periodization (D'Andrea 2012, 2020; Shalev et al. 2022), it still cannot tell us much about IBA burials chronology. Radiocarbon absolute dating is a potential tool to explore IBA burials chronology. The best practice in bone radiocarbon dating is isolating and dating the collagen fraction within the bone (Yizhaq et al. 2005; Brock et al. 2010). Unfortunately, human bones from ancient tombs in the southern Levant often undergo considerable diagenesis due to climatic and environmental conditions in this region. Bones are often found fragmented and in a deteriorated condition, and many times there is below minimal content or insufficient quality of collagen to enable trustable radiocarbon dating. In most of the IBA burials excavated in Israel during the last several decades, human bones were not preserved well or not researched.

Nevertheless, in the presented research, we succeeded in dating IBA human bones from several IBA burial sites, sampling bones during new excavations of IBA burials, and sampling stored IBA bones from a few past excavations.

https://doi.org/10.1017/RDC.2022.58 Published online by Cambridge University Press

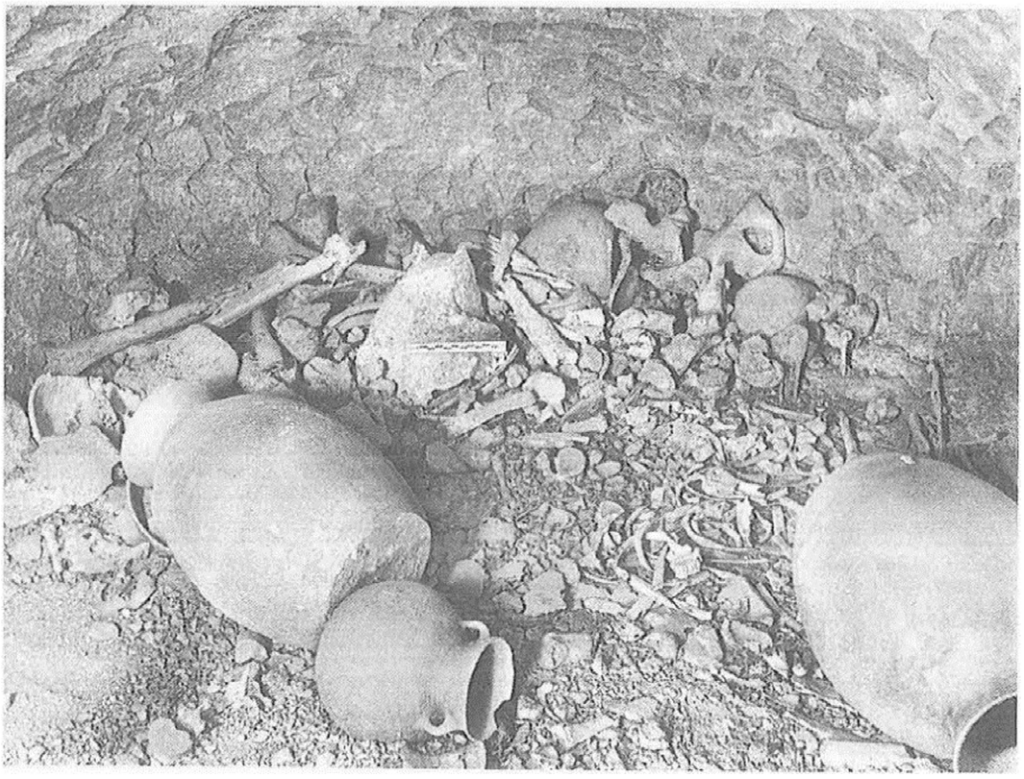

Figure 3 Jebel-Qaaqir. Tomb B-54 chamber B with its contents (photo source: Dever 2014: fig.2.54).

MATERIALS AND METHODS

Sites Sampled for IBA Burials Dating

A human skeleton within a single-phase burial cave is a safe and secure context for radiocarbon dating the tomb's contents. The first ^{14}C dates of human bones published from IBA burial sites in Israel are presented here. These ^{14}C dates are all of human bones found within well verified IBA contexts within the following burial sites (see circled sites in Figure 1):

- Jebel-Qaaqir
- Yehud
- Sheikh-Danon
- Kefar-Veradim
- Hazorea

The following sections present the bone sampling details for each of the above sites:

Jebel Qaaqir

In cemetery B at Jebel Qaaqir, 59 tombs were excavated by W. Dever (Dever 2014). Most of them were robbed in antiquity, but a few seemed intact. Sealed tomb B-54 with its two chambers (A, B) is one of the richest caves found at Jebel Qaaqir (Figure 3). Disarticulated human bones of at least nine individuals, five females and four males, were identified in

https://doi.org/10.1017/RDC.2022.58 Published online by Cambridge University Press

Figure 4 Partial view of a typical IBA tomb (L226) excavated at Yehud burial ground. Note the pottery offerings and small copper items inside the four-spouted lamp. (Photo courtesy of Yehuda Govrin.)

tomb B-54. Seven were adults 40 to 60 years old, and two were adolescents (Smith 1982). Three bronze objects and ten intact ceramic vessels were found in this tomb and identified as IBA-related. Bones from this tomb were sampled from the NNH collections at the Hebrew University with permission from P. Smith. We have chosen and dated five left-side radii and a rib that showed sufficient collagen preservation, thus ensuring we dated five different individuals. However, we could not associate each dated bone to a specific individual.

Yehud Burial Ground

Salvage excavations of burial grounds at Yehud, including over 100 IBA single shaft tombs and several MB shaft tombs, were directed by Yehuda Govrin on behalf of the Hebrew Union College during 2008/2009 (Govrin 2015) and 2012 (Govrin forthcoming). The 2012 excavation uncovered a field of shaft tombs dug into the natural *Hamra* soil. Most tombs, including all those dated in this research, contained a single human skeleton in articulation and several distinctive IBA ceramic vessels (Figure 4). Some other tombs were identified as from the MB period according to their pottery. Bones from the Yehud burial field were documented and stored. Systematic collagen tests over bone fragments from the 2012-season excavated IBA shaft tombs were performed. Overall, 149 bone samples from 52 IBA tombs were tested to assess their suitability for ^{14}C dating. Bones from fourteen (14) IBA tombs included suitable collagen and were radiocarbon dated. Thirteen dated bones are from the main burials concentration. Dated sample RTD-8948 from tomb L2000 was located in a smaller tomb concentration, abutting the main burial field from the southwest.

https://doi.org/10.1017/RDC.2022.58 Published online by Cambridge University Press

Figure 5 Sheikh Danon. A view of the burial cave main chamber from its entry point during excavation, looking south. The corridor into the smaller chamber is seen at the back. (Photo courtesy of Ron Lev.)

Sheikh Danon

Salvage excavations led by Zach Horowitz on behalf of the Israel Antiquities Authority were conducted during the winter of 2018 in a burial cave on the northern slopes of the village of Seikh Danon on Israel's northern coastal plain, five km East of Nahariya (permit 8212/18. To be published). The cave appears to be a part of an IBA burial ground in that location (Getzov 2008). The excavated cave consists of two rectangular rooms. A rectangular entry shaft leads into the main chamber, with a smaller room as its extension. Over 40 complete pottery vessels, a few copper alloy objects, and disarticulated scattered Human bones of at least ten individuals were unearthed within ~40 cm of accumulated sediment and collapsed ceiling debris on the bottom of this cave's two rooms (Figure 5). All material culture found was identified as belonging to the IBA period. Several human bones from various locations in the cave entry room were collected for ^{14}C dating, and three bones that displayed sufficient Collagen amounts were processed and dated. The dated bone fragments were collected at least two meters apart. Yet, the bones in this cave were disarticulated and scattered around, and we are not sure if they represent different individuals.

Kefar Veradim

Salvage excavation of burial ground containing at least 20 shaft tombs was conducted in 2016–2018 by Edwin C.M. van den Brink at Kefar Veradim on behalf of the IAA (Van Den Brink 2020). This burial site is about 1.5 km west of the Kfar-Vradim IBA rural

https://doi.org/10.1017/RDC.2022.58 Published online by Cambridge University Press

Figure 6 Kefar Veradim. Shaft 125 and the entrance to Burial Chamber 142, looking east. (Photo source: Van Den Brink 2020: Fig. 2.)

settlement (Covello-Paran 2020). In shaft tomb chamber L142 (Figure 6), disturbed human bones were located alongside an IBA jar fragment and a few copper/bronze elements. A human long-bone fragment from this chamber (labeled L142-a) was radiocarbon dated.

Hazorea

The IBA cemetery discovered in the southern part of Kibbutz Hazorea in the Jezreel Valley was excavated periodically between the 1950s and the 1980s by E. Anati and E. Meyerhof (Meyerhof 1989; see also Covello-Paran 2015:226–241). Human bones from tomb-3 at Hazorea (Figure 7) were located at the IAA storage facility. Two bones were tested positive for suitable collagen and were radiocarbon dated (Lev et al. 2021). The two dated bone fragments were found in separate bone accumulations within separate rooms and most probably belonged to different individuals.

Preparation of Bone Samples

Potential bones/teeth material for dating found within excavation was collected in aluminum foil envelopes. Bones from IBA tombs located in excavation storages were verified to be with no treatment, gluing, or preservation activities following their excavation. Sufficient collagen preservation is required in the bone (or the tooth dentine) to be a candidate for radiocarbon dating. The verification involved "prescreening" of the bone to assess the probability of collagen preservation by FTIR (Fourier transformed infrared spectroscopy) SF (splitting factor) indication (Weiner et al. 1990), followed by another prescreening test for collagen existence on 200 mg of powdered bone which is pretreated with 1N HCl acid to dissolve the bone apatite. If the FTIR spectrum of the bone/tooth insoluble fraction indicates a good collagen signal, then the bone is a probable candidate for radiocarbon dating. Chosen bones for dating went through a collagen extraction and purification procedure

https://doi.org/10.1017/RDC.2022.58 Published online by Cambridge University Press

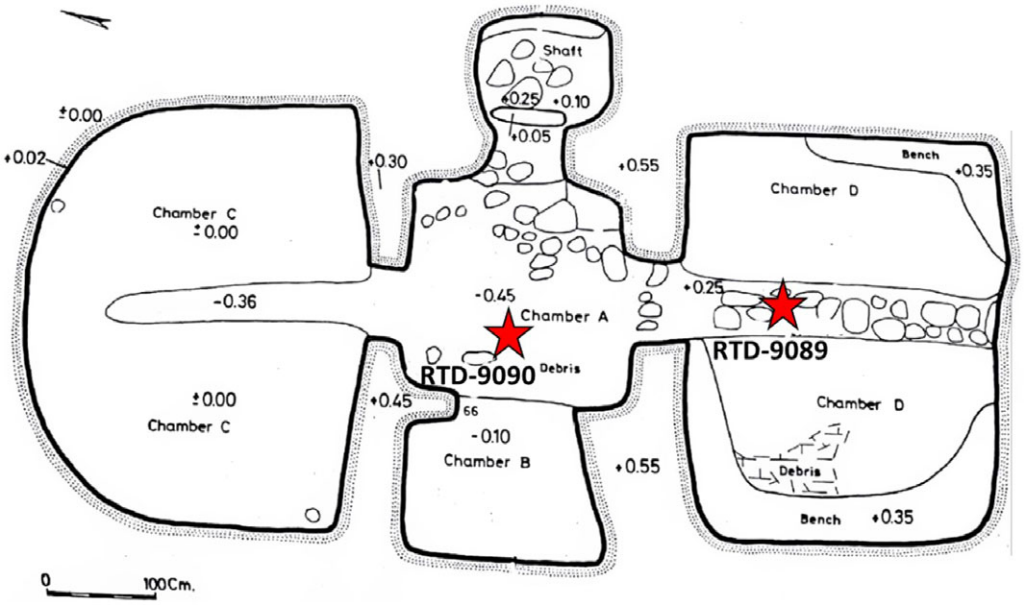

Figure 7 Plan of tomb-3 at Hazorea, where the dated bones documented find locations are marked by stars. (Plan based on Meyerhof 1989: Figure 7.)

(Yan et al. 2021). In the hot and humid Mediterranean regions, bone preservation is usually low after being buried in sediment for thousands of years. Screening techniques were enhanced to validate the dating suitability of bones with collagen W% < 1%, including 35 wt% as the minimal accepted presence of carbon in the extracted collagen and careful comparison of the extracted collagen FTIR spectrum with that of collagen standard.

Combustion and Graphitization

Combustion and graphitization of bone samples up to RTD-9292 were done at the Kimmel Center for Archaeological Science lab, Weizmann Institute of Science. The pretreated samples were combusted to CO_2 in vacuumed quartz tubes with 200 mg of copper oxide by heating to 900°C for 200 min. The CO_2 was reduced to graphite using 2 mg Fe powder as a catalyst and hydrogen and heated to 600°C for 20 hr.

Pretreated samples after RTD-9292 were combusted and graphitized by the new Vario Isotope Select Elemental Analyzer (EA), coupled with AGE-3 graphitization system (Wacker et al. 2010), at D-REAMS, Weizmann Institute of Science. Pretreated samples weighed in tin cups were dropped into the EA combustion tube wherein the presence of external oxygen flash combustion occurred at a temperature of 950°C. CO_2 was separated from the rest of the gaseous combustion products and transferred by Helium carrier gas into the AGE-3 graphitization unit, where carbon was converted to graphite through reduction by hydrogen over iron as catalyst. Carbon and nitrogen concentrations are measured to determine C/N atomic ratio and carbon weight percentage in the collagen (Van Klinken 1999).

https://doi.org/10.1017/RDC.2022.58 Published online by Cambridge University Press

Table 1 Total number of sampled bones from each burial site and the number of bones with sufficient amount and quality of collagen that were dated.

Burial site	Sampled bones #	Dated bones #	Datable bones %	Sediment composition
Qanat el Jaar	16	0	0	Moist sediment
Yehud	149	14	9	Cemented Hamra (quartz and clay) soil
Hazorea	8	2	25	Clay
Sheikh Danon	10	3	30	Partially covered in clay
Jebel Qaaqir	12	6	50	On limestone surface
Kefar Veradim	1	1	—	Clay and carbonate minerals
Total	196	26	13	

^{14}C Measurement

The graphite ^{14}C content was measured by the D-REAMS accelerator at the Weizmann Institute of Science (Regev et al. 2017). Radiocarbon ages were reported in conventional radiocarbon years BP (Before Present, where "present" is defined as the year 1950) following international conventions (Stuiver et al. 1977). All calculated ^{14}C ages have been corrected for the isotopic fractionation to be equivalent to the standard of δ^{13}C value of –25‰. The radiocarbon ages were calibrated using the OxCal 4.4 online version (https://c14.arch.ox.ac.uk/oxcal/OxCal.html) and the IntCal 20 calibration curve (Reimer et al. 2020).

RESULTS

Preservation of Bones

The percentage of dated bones in each site is presented in Table 1. The chemical parameters of the dated bones are shown in Table 2. The extent of collagen preservation within ancient bones (verified by SF, FTIR, and element ratios) appears to depend on the local environment of the bones resting place. Moist sediments, as in Qanat el Jaar and Yehud, seem to be a non-favorable environment for collagen preservation. The collagen better preserves in dry, arid environments, as in Jebel Qaaqir or Sheikh Danon. We also found that some bones sampled from the same tomb or adjacent tombs only one meter apart proved to have different collagen preservation. For example, in Yehud burial ground, tomb L269 bone insoluble fraction presented a good FTIR collagen signal, while adjacent tomb L270 did not (Figure 8).

SF was shown to be an effective indicator for insufficient (low amount) collagen in the bones sampled in this research. Of the bones, 50% had SF > 3.3. None of the bones with SF > 3.3 had sufficient collagen for dating (Figure 9). On the other hand, SF below the value of 3.3 by itself could not predict sufficient collagen as only 26 bones out of 96 tested bones that showed SF < 3.3 proved to have sufficient collagen and were dated (27% of the bones with SF < 3.3). Thus, only if the FTIR spectrum of the insoluble fraction of the bone/tooth sample after HCl treatment presented clear collagen absorbance peaks, then the sample was considered a candidate for further processing towards radiocarbon dating. The SF ratio tests on bones from different IBA burial sites show a similar bone diagenesis pattern. The bones with sufficient collagen for dating present 2.6 < SF < 3.3, regardless of the FWHM (Asscher et al. 2011).

https://doi.org/10.1017/RDC.2022.58 Published online by Cambridge University Press

Table 2 Details and preservation parameters of the dated IBA bones.

Site	Sample number	Field ID	SF	Eff. W %	C %	C/N	Gender	Person age estimation
Sheikh Danon	RTD-9434	SD L2100-e	2.91	0.77	42.91	3.23	n.d.	n.d.
	RTD-9433	SD L2100-c	2.96	3.88	43.87	3.23	M	Above 30
	RTD-9755	SD L2100-b	3.19	1.70	44.13	3.25	n.d.	n.d.
Hazorea	RTD-9089	T-III b	n.d.*	1.51	43.26	3.27	n.d.	n.d.
	RTD-9090	T-III c	n.d.	1.82	43.24	3.22	n.d.	n.d.
Yehud	RTD-8948	L2000a	2.68	0.78	n.d.	n.d.	M	40–45
	RTD-9292	L167 a-2	3.15	1.01	42.70	3.25	n.d.	Above 40
	RTD-9293	L269 d	n.d.	0.74	n.d.	3.28	M	30
	RTD-8928	L215b	2.89	0.13	n.d.	n.d.	M	35–45
	RTD-9075	L257a-2	3.17	0.27	41.67	3.24	F	30–40
	RTD-8927	L211b	2.75	1.61	39.86	3.25	F	25–35
	RTD-8931	L267a	2.67	1.17	42.44	3.27	M	20–30
	RTD-8947	L1010b	2.71	0.70	39.00	3.24	n.d.	n.d.
	RTD-8926	L161a	2.97	0.39	41.94	3.30	M	35–45
	RTD-8917	L733c	2.72	0.52	42.88	3.25	n.d.	20–30
	RTD-8913	L152c	2.95	0.31	36.82	3.35	M	Above 50
	RTD-8930	L250b	3.11	0.07	40.00	3.32	M	15–16
	RTD-8692	L162c	2.89	0.20	35.40	n.d.	M	25–35
	RTD-8946	L248c	2.86	0.14	35.00	n.d.	M	Above 50
Kefar Veradim	RTD-9756	L142	n.d.	0.16	43.55	3.39	n.d.	n.d.
Jebel Qaaqir	RTD-9076	B54A-1541-2	2.84	2.80	43.44	3.22	n.d.	n.d.
	RTD-9007	B54A-1505	2.82	2.08	40.20	3.25	n.d.	n.d.
	RTD-9291	B54B-d	n.d.	2.19	39.80	n.d.	n.d.	n.d.
	RTD-9077	B54A-1542	2.76	0.16	38.00	n.d.	n.d.	n.d.
	RTD-9009	B54A-1544	3.04	2.24	43.00	3.27	n.d.	n.d.
	RTD-9010	B54B-b	3.04	0.70	42.68	3.30	n.d.	n.d.

*n.d. stands for "no data."

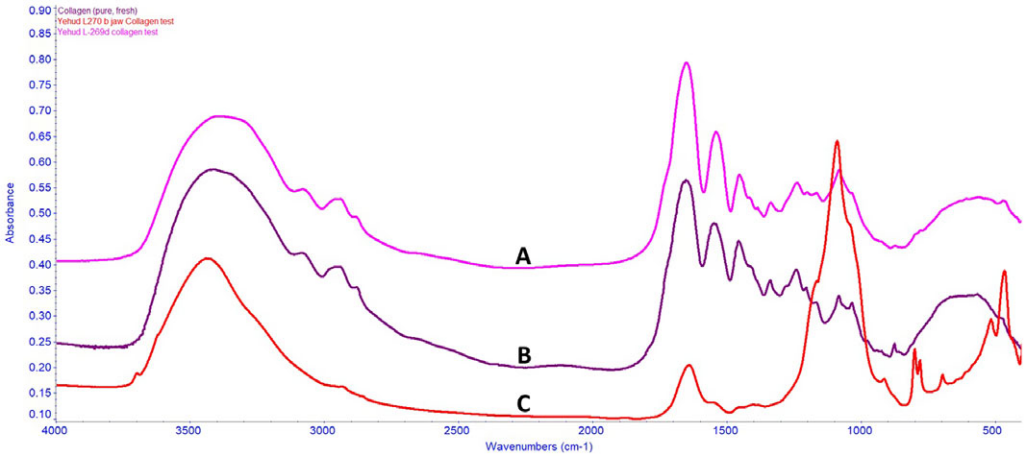

Figure 8 Comparative FTIR spectra of the following samples: (A) Typical bone insoluble fraction showing good collagen preservation (dated bone L269d RTD-9293) for the samples in this study. (B) Standard sample of fresh collagen. (C) Bone insoluble fraction showing poor collagen preservation (bone L270b, not dated). Note the typical collagen FTIR peaks at 1640, 1550, and 1450 cm^{-1} in both spectra A and B (See also Weiner 2010: Fig. 12.19), and the different spectrum C that is dominated by characteristic quartz absorbance peaks (prominent peak at 1084 cm^{-1}), with only a low signal of organic compounds.

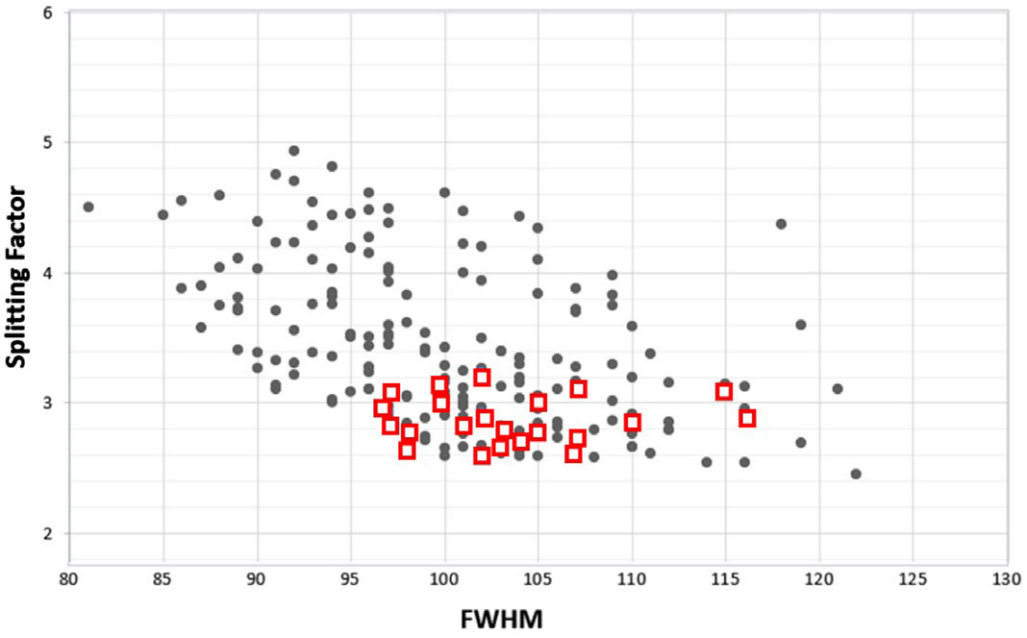

Figure 9 FTIR "Splitting Factor" test results on bones from four different IBA burial sites (Yehud, Jebel-Qaaqir, Sheikh-Danon, Qanat-el-Jaar). Squares mark bones that later proved to have sufficient collagen and were dated. Dots are bones that did not have adequate collagen for dating. FWHM stands for the FTIR Full Width at Half Maximum height of the 1035 cm^{-1} peak of carbonated hydroxyapatite (Asscher et al. 2011).

https://doi.org/10.1017/RDC.2022.58 Published online by Cambridge University Press

Bone-Dating Results

The dates presented here (Table 3, Figure 10) are the first radiocarbon dates of human bones published from IBA burial sites in the southern Levant. The two Hazorea tomb-3 dates above were also presented recently elsewhere (Lev et al. 2021). The dated bones were all found within well verified IBA burial contexts, accompanied by typical IBA burial goods.

DISCUSSION

IBA Shaft Burials Dating

The dated human bones in this research originated in shaft tombs of five different sites from various regions in Israel: from Jebel Qaaqir in the southern Judean hill region and up to Kefar Veradim in upper Galilee (Figure 1). The measured date ranges cover most of the IBA timeframe: bones' date-range medians span from the 25th century BCE, through IBA central dates and up to the beginning of the 20th century BCE. This sample of burials follows the same chronological pattern presented by the absolute dating of IBA settlements in the southern Levant (Regev et al. 2012; D'Andrea 2014: Chapter 2; Lev 2020: Chapter 8). Thus, the current research shows evidence for a parallel chronological range of IBA settlements and IBA burials, supporting an observation that the IBA signature shaft tomb burials are a fundamental part of the IBA culture from start to end, alongside its other characteristic material culture.

IBA Collective Burials

The dates from bones belonging to five out of at least nine individuals counted in one shaft tomb labeled B54 at Jebel Qaaqir (Dever 2014:32–33) were presented above (Table 3). The dated bones produced a sufficient amount of good quality collagen, as validated by the FTIR spectra and the chemical analysis (see Table 2). The calibrated date range medians of Tomb B54 bones span from around 2300 BCE to 2000 BCE, presenting for the first time a single IBA shaft tomb that contains human remains accumulated through generations and spanning over a few hundred years. The Jebel Qaaqir dates indicate a tribal, lineage, or family-oriented community with long-lasting tradition reflected in ongoing collective burial practice, as seen in tomb B54. The phenomenon of a few generations gap between individuals buried in the same tomb was also observed at Seikh Danon (Table 3). Another common feature in these collective burials is scattered and disarticulated partial skeletons, including mainly larger bones, thus suggesting secondary burials or moving aside old bones when adding remains of new people to the chamber.

Yehud Burial Ground Observations

The dating results from the Yehud IBA burial site show that it was active during IBA for over a century, keeping the same burial tradition and style. In the burials, the dead were laid in similar positions in the same type of shaft tombs dug until the boundary between the *Hamra* soil and the yellow sand layer below it. Similar burial goods were found in the tombs, including (mainly) jars, cups, and open bowls. Tombs with earlier calibrated date range medians (before 2230 BCE) were sampled from the eastern part of the field (except for RTD-9292), and those with later calibrated date range medians (after 2230 BCE) were sampled from the western part (except for RTD-8930), suggesting an expansion of the burial field from east to west through time (Figure 11). Many shafts were dug into the local Hamra soil, some are very close, yet the tombs did not cut each other. The above observations suggest that the IBA

https://doi.org/10.1017/RDC.2022.58 Published online by Cambridge University Press

Table 3 Radiocarbon date ranges of human bones from IBA burial grounds across Israel. Within each site, samples are ordered by their radiocarbon date.

Sample number	Field ID	Material	^{14}C age ±1σ year BP	Calibrated range ±1σ BCE	Calibrated range ±2σ BCE
Sheikh Danon					
RTD-9434	L2100-e	Human longbone	3940±41	2549 (4.3%) 2538 2490 (46.7%) 2399 2383 (17.2%) 2347	2568 (14.1%) 2518 2500 (81.3%) 2299
RTD-9433	L2100-c	Human cranium	3929±41	2477 (46.9%) 2391 2386 (21.3%) 2346	2566 (7.8%) 2524 2497 (87.6%) 2293
RTD-9755	L2100-b	Human longbone	3767±14	2204 (15.0%) 2192 2179 (53.2%) 2143	2277 (9.7%) 2253 2228 (0.7%) 2224 2210 (85.0%) 2137
Hazorea					
RTD-9089	T-3 b	Human longbone	3817±25	2292 (68.3%) 2204	2398 (1.6%) 2385 2345 (87.8%) 2196 2173 (6.0%) 2146
RTD-9090	T-3 c	Human femur	3807±19	2286 (36.6%) 2247 2237 (31.6%) 2204	2336 (1.3%) 2327 2299 (85.7%) 2196 2173 (8.5%) 2146
Yehud					
RTD-8948	L2000a	Human tibia	3829±27	2335 (5.2%) 2324 2307 (24.6%) 2267 2261 (38.3%) 2206	2456 (4.0%) 2418 2407 (5.1%) 2376 2351 (85.0%) 2198 2165 (1.4%) 2152
RTD-9292	L167a-2	Human longbone	3827±25	2332 (2.6%) 2327 2300 (65.6%) 2206	2436 (1.4%) 2420 2405 (3.7%) 2378 2350 (88.9%) 2197 2166 (1.4%) 2151
RTD-8150	L269d	Human longbone	3815±24	2289 (18.6%) 2267 2261 (49.6%) 2206	2344 (91.2%) 2196 2171 (4.2%) 2147

(Continued)

Table 3 (*Continued*)

Sample number	Field ID	Material	^{14}C age ±1σ year BP	Calibrated range ±1σ BCE	Calibrated range ±2σ BCE
RTD-8928	L215b	Human humerus	3812±30	2295 (68.2%) 2201	2401 (1.9%) 2382 2348 (84.2%) 2189 2182 (9.2%) 2141
RTD-9075	L257a-2	Human tibia	3810±20	2286 (68.2%) 2206	2335 (1.4%) 2325 2307 (90.0%) 2197 2169 (4.0%) 2149
RTD-8927	L211b	Human humerus	3810±26	2287 (68.2%) 2206	2342 (87.9%) 2194 2176 (7.5%) 2144
RTD-8931	L267a	Human longbone	3807±27	2287 (68.2%) 2204	2343 (84.9%) 2191 2181 (10.5%) 2142
RTD-8947	L1010b	Human longbone	3797±36	2290 (57.7%) 2197 2169 (10.5%) 2148	2429 (0.3%) 2425 2402 (1.5%) 2382 2349 (92.4%) 2133 2080 (1.2%) 2061
RTD-8926	L161a	Human longbone	3789±30	2285 (26.6%) 2247 2235 (25.8%) 2196 2171 (15.7%) 2146	2337 (1.3%) 2323 2309 (94.1%) 2135
RTD-8917	L733c	Human humerus	3776±27	2278 (17.4%) 2252 2229 (3.6%) 2222 2211 (15.4%) 2190 2182 (31.8%) 2142	2291 (93.4%) 2133 2078 (2.0%) 2062
RTD-8913	L152c	Human humerus	3767±37	2280 (14.6%) 2250 2231 (4.8%) 2219 2213 (48.8%) 2136	2296 (82.7%) 2116 2099 (12.7%) 2038
RTD-8930	L250b	Human humerus	3762±26	2268 (4.4%) 2260 2206 (63.8%) 2138	2285 (14.0%) 2247 2235 (73.6%) 2129 2087 (7.8%) 2049
RTD-8692	L162c	Human tooth	3758±34	2275 (8.4%) 2256 2209 (53.6%) 2134 2079 (6.2%) 2063	2288 (79.9%) 2120 2095 (15.5%) 2041

Table 3 (*Continued*)

Sample number	Field ID	Material	^{14}C age ±1σ year BP	Calibrated range ±1σ BCE	Calibrated range ±2σ BCE
RTD-8946	L248c	Human humerus	3751±26	2204 (65.5%) 2135 2070 (2.7%) 2065	2279 (7.1%) 2250 2230 (1.4%) 2221 2212 (70.1%) 2121 2094 (16.9%) 2042
Kefar Veradim					
RTD-9756	L142-a	Human longbone	3772±14	2266 (4.0%) 2261 2206 (15.8%) 2193 2178 (48.5%) 2144	2278 (14.9%) 2251 2229 (2.0%) 2222 2211 (78.5%) 2138
Jebel Qaaqir					
RTD-9076	B54A-1541-2	Human radius bone	3846±19	2346 (52.2%) 2279 2250 (12.4%) 2230 2220 (3.6%) 2212	2456 (6.5%) 2418 2406 (9.0%) 2376 2351 (56.7%) 2268 2260 (23.2%) 2206
RTD-9007	B54A-1505	Human radius bone	3755±23	2201 (68.2%) 2140	2279 (7.1%) 2251 2229 (1.2%) 2221 2211 (76.4%) 2127 2089 (10.8%) 2047
RTD-9291	B54B-d	Human rib bone	3750±23	2203 (68.2%) 2136	2277 (5.0%) 2253 2228 (0.5%) 2224 2210 (73.7%) 2122 2093 (16.3%) 2042
RTD-9077	B54A-1542	Human radius bone	3743±20	2200 (66.2%) 2135 2068 (2.0%) 2065	2267 (0.7%) 2261 2206 (73.8%) 2122 2093 (21.0%) 2042
RTD-9009	B54A-1544	Human radius bone	3683±31	2135 (43.4%) 2070 2065 (24.8%) 2028	2194 (2.8%) 2177 2145 (92.6%) 1966
RTD-9010	B54B-b	Human radius bone	3631±25	2027 (68.2%) 1958	2122 (6.7%) 2093 2042 (88.7%) 1920

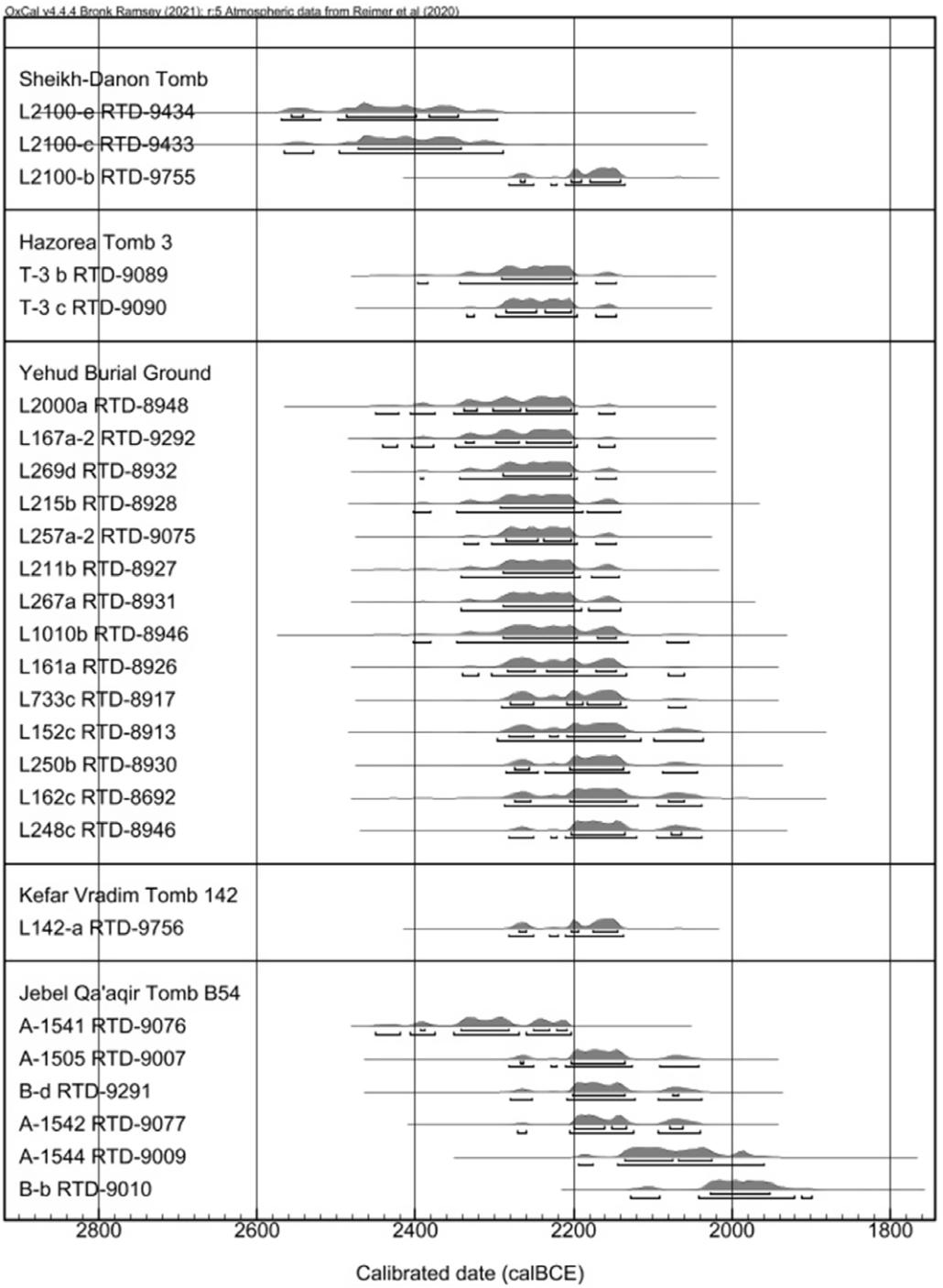

Figure 10 Calibrated range probability distributions of bone samples from IBA burial grounds in Israel. Sample field identification is listed on the left, followed by their lab number. Within each site, samples are ordered according to their radiocarbon date.

https://doi.org/10.1017/RDC.2022.58 Published online by Cambridge University Press

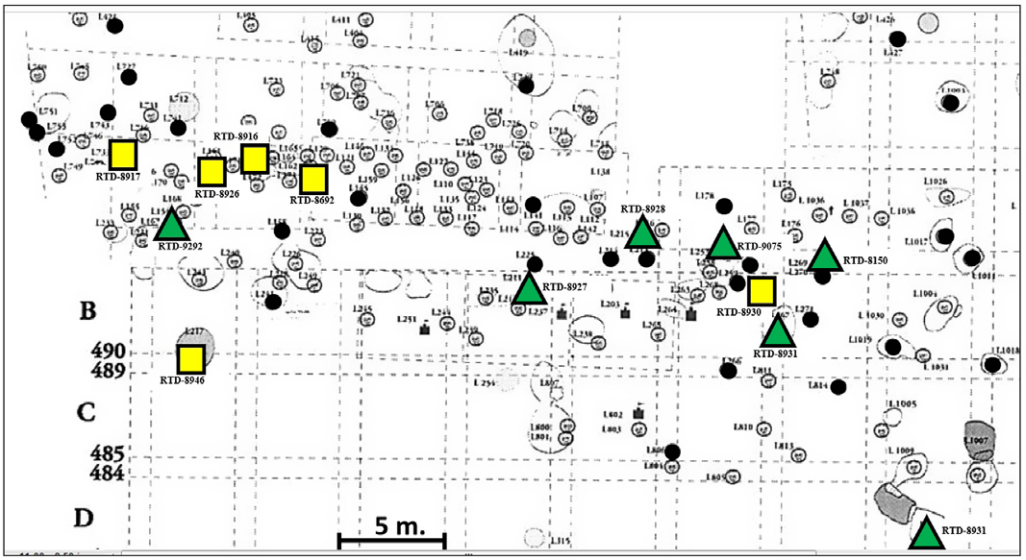

Figure 11 Partial schematic plan of Yehud main area tombs spatial distribution. Triangles mark tombs that produced earlier calibrated distribution ranges (mean before 2230 BCE). Squares mark tombs that produced later calibrated distribution ranges (mean after 2230 BCE). The related sample number is displayed by each dated tomb. Black marked tombs were sampled but had insufficient collagen for dating. Non-colored tombs were not sampled.

people knew the location of the tombs at the Yehud burial ground, including those from past generations. They kept the burial traditions very similar for over a century, and as the burial area became crowded, they extended the burial field to the west. Such behavior suggests a long-standing social organization that keeps standard and orderly burial practices for several generations.

CONCLUSION

This research performed the first absolute dating measurements on Intermediate Bronze Age human remains from southern Levant burial sites. The measured date ranges cover most of the IBA timeframe, demonstrating that the signature shaft tomb burials were integrated into the IBA culture throughout its entire lifespan. Collective burial in the same shaft tomb supplied dates centuries apart between the humans buried in that tomb. This phenomenon suggests a traditional tribal or familial community with long-term cultural memory as reflected in their burial traditions. The conservative nature of the IBA culture is also apparent in tombs quarried for over a century at Yehud with identical structures and the same burial arrangement. The above findings complement previous observations that the same pottery types and metal tools are found in contexts dated throughout half a millennium of the IBA. The overall emerging picture is of a very conservative rural community, keeping its rigid way of life and its traditions for many centuries.

Further radiocarbon dating of IBA burials with their rich pottery assemblages also holds promising potential for improving the IBA pottery chronology precision.

https://doi.org/10.1017/RDC.2022.58 Published online by Cambridge University Press

ACKNOWLEDGMENTS

We wish to thank Patricia Smith (Faculty of Dental Medicine, Hebrew University of Jerusalem) for helping us identify relevant bone samples for radiocarbon dating from Jebel Qaaqir burial cave B54. We also thank Edwin van den Brink (Israel Antiquities Authority) for a bone sample for radiocarbon dating from the Kefar Veradim IBA burial tomb L142.

The Exilarch Foundation supported the Radiocarbon research for the Dangoor Research Accelerator Mass Spectrometer (D-REAMS) Laboratory. We wish to thank the Kimmel Center for Archaeological Science and George Schwartzman Fund for funding support to R.L., laboratory, and material analysis. E.B. is the incumbent of the Dangoor Professorial Chair of Archaeological Sciences at the Weizmann Institute of Science.

REFERENCES

Al-Muheisen Z, Al-Bashaireh K. 2012. AMS radiocarbon determination and cultural setting of the vertical shaft tomb complex at Tell al-Husn, Irbid, Northern Jordan. Palestine Exploration Quarterly 144(2):84–101.

Asscher Y, Weiner S, Boaretto E. 2011. Variations in atomic disorder in biogenic carbonate hydroxyapatite using the infrared spectrum grinding curve method. Advanced Functional Materials 21(17):3308–3313.

Van Den Brink ECM. 2020. Kefar Veradim. Hadashot Arkheologiyot 132.

Brock F, Higham T, Ditchfield P, Bronk Ramsey C. 2010. Current pretreatment methods for AMS radiocarbon dating at the Oxford Radiocarbon Accelerator Unit (ORAU). Radiocarbon 52(1):103–112.

Covello-Paran K. 2015. The Jezreel Valley during the Intermediate Bronze Age: social and cultural landscapes [unpublished PhD thesis].

Covello-Paran K. 2020. Excavations at Kfar Vradim and Intraregional Settlement Patterns of the Western Upper Galilee During the Intermediate Bronze Age. In: Richard S, editor. New horizons in the study of the Early Bronze III and Early Bronze IV of the Levant. University Park: Eisenbrauns. p. 376–394.

D'Andrea M. 2012. The Early Bronze IV period in south-central Transjordan: reconsidering chronology through ceramic technology. Levant 44(1):17–50.

D'Andrea M. 2014. The Southern Levant in Early Bronze IV: issues and perspectives in the pottery evidence. Rome.

D'Andrea M. 2020. About stratigraphy, pottery, and relative chronology: some considerations for a refinement of the archaeological periodization of the southern Levantine Early Bronze Age IV. In: Richard S, editor. New horizons in the study of the Early Bronze III and Early Bronze IV of the Levant. University Park: Eisenbrauns. p. 395–416.

Dever WG. 1972. Middle Bronze Age I cemeteries at Mirzbâneh and 'Ain-Sâmiya. Israel Exploration Journal 22(2/3):95–112.

Dever WG. 2014. Excavations at the Early Bronze IV sites of Jebel Qa'aqir and Be'er Resisim. Winona Lake.

Epstein C. 1985. Dolmans excavated in the Golan. 'Atiqot 17 (ES):20–58.

Fall PL, Falconer SE, Höflmayer F. 2021. New Bayesian radiocarbon models and ceramic chronologies for Early Bronze IV Tell Abu en-Ni'aj and Middle Bronze Age Tell el-Hayyat, Jordan. Radiocarbon 63(1):41–76.

Getzov N. 2008. Sheikh Danon, Esh-Sheikh Dawud. Hadashot Arkheologiyot 120.

Govrin Y. Excavations at Yehud – the 2012 season. NGSBA Archaeology (Forthcoming).

Govrin Y. 2015. Excavations at Yehud – the 2008–2009 seasons. NGSBA Archaeology 3:1–160.

Guy PL. 1938. Megiddo tombs. Chicago: Oriental Institute Publications.

Helms S. 1983. The EB IV (EB-MB) Cemetery at Tiwal esh-Sharqi in the Jordan Valley, 1983. Annual of the Department of Antiquities of Jordan. p. 55–85.

Helms S, McCreery D. 1988. Helms and McReery 1988 – rescue excavations at Umm el-Bighal – the pottery. Annual of the Department of Antiquities of Jordan. p. 319–348.

Höflmayer F, Dee MW, Genz H, Riehl S. 2014. Radiocarbon evidence for the Early Bronze Age Levant: the site of Tell Fadous-Kfarabida (Lebanon) and the end of the Early Bronze III Period. Radiocarbon 56(2):529–542.

Horowitz, Z. 2016. The Intermediate Bronze Age tombs. In: Yannai E, editor. 'En Esur ('Ein Asawir) II: excavations at the cemeteries. Jerusalem: Israel Antiquities Authority. p. 127–187.

Ilan D. 2002. Mortuary practices in early Bronze Age Canaan. Near Eastern Archaeology 65(2):92–104.

https://doi.org/10.1017/RDC.2022.58 Published online by Cambridge University Press

Kennedy MA. 2015. EB IV stone-built CIST-graves from sir flinders Petrie's excavations at Tell el-'Ajjul. Palestine Exploration Quarterly 147(2):104–129.

Kenyon KM. 1965. Excavations at Jericho II: the tombs excavateed in 1955–1958. London: British School of Archaeology in Jerusalem.

Van Klinken GJ. 1999. Bone collagen quality indicators for palaeodietary and radiocarbon measurements. Journal of Archaeological Science 26(6):687–695.

Lapp P. 1966. The Dhahr Mirzbaneh Tombs : three intermediate Bronze Age cemeteries in Jordan. New Haven.

Lev R. 2020. Absolute chronology for the Intermediate Bronze Age culture in the southern Levant [PhD thesis]. Rehovot: Weizmann Institute of Science.

Lev R, Bechar S, Covello-Paran K, Boaretto E. 2021. Absolute chronology of the Black Wheel Made Ware in the Southern Levant and its synchronization with the Northern Levant. Levant 53(2):151–163.

Lev R, Shalev O, Paz Y, Regev J, Boaretto E. 2020. Bridging the Gap EBIII-IBA: Early Intermediate Bronze radiocarbon dates from Khirbat el-'Alya Northeast, Israel. Radiocarbon 62(6):1637–1649.

Mazar A. 1990. Archaeology of the land of the Bible: 10,000–586 B.C.E. Yale University Press.

Meyerhof EL. 1989. The Bronze age necropolis at Kibbutz Hazorea, Israel. BAR International Series.

de Miroschedji P. 2009. Rise and collapse in the Southern Levant in the Early Bronze Age. Scienze dell'antichità. Storia Archeologia Antropologia 15:101–129. Roma: Universita Degli Studi di Roma – La Sapienza.

Oren ED. 1973. The Northern Cemetery of Beth Shan. Leiden: Brill.

Prichard J. 1963. The Bronze Age cemetery at Gibeon. Philadelphia.

Regev J, de Miroschedji P, Greenberg R, Braun E, Greenhut Z, Boaretto E. 2012. Chronology of the Early Bronze Age in Southern Levant: new analysis for a high chronology. Radiocarbon 54(3–4):525–566.

Regev J, Finkelstein I, Adams MJ, Boaretto E. 2014. Wiggle-matched ^{14}C chronology of Early Bronze Megiddo and the synchronization of Egyptian and Levantine chronologies. Agypten und Levante 24:243–266.

Regev L, Steier P, Shachar Y, Mintz E, Wild EM, Kutschera W, Boaretto E. 2017. D-REAMS: a new compact AMS system for radiocarbon measurements at the Weizmann Institute of Science, Rehovot, Israel. Radiocarbon 59(3):775–784.

Reimer PJ, Austin WEN, Bard E, Bayliss A, Blackwell PG, Ramsey CB, Butzin M, Cheng H, Edwards RL, Friedrich M, Grootes PM, Guilderson TP, Hajdas I, Heaton TJ, Hogg AG, Hughen KA, Kromer B, Manning SW, Muscheler R, Palmer JG, Pearson C, van der Plicht J, Reimer RW, Richards DA, Scott EM, Southon JR, Turney CSM, Wacker L, Adolphi F, Büntgen U, Capano M, Fahrni SM, Fogtmann-Schulz A, Friedrich R, Köhler P, Kudsk P, Miyake F, Olsen J, Reinig F, Sakamoto M, Sookdeo A, Talamo S. 2020. The IntCal20 Northern Hemisphere radiocarbon age calibration curve (0–55 cal kBP). Radiocarbon 62(4):725–757. doi: 10.1017/RDC.2020.41.

Richard S, Long Jr. JC, Holdorf PS, Peterman G, editors. 2010. Khirbet Iskander: final report on the Early Bronze IV Area C 'Gateway' and cemeteries. Boston: ASOR.

Shalev O, Walzer N, Paz Y. 2022. The EBA–IBA transition in the Judean Shephelah – a view from the IBA. In: Adams MJ, Roux V, editors. Transitions during the Early Bronze Age in the Levant – methodological problems and interpretative perspectives. Münster: Zaphon. p. 285–300.

Sharon G, Barash A, Eisenberg-Degen D, Grosman L, Oron M, Berger U. 2017. Monumental megalithic burial and rock art tell a new story about the Levant Intermediate Bronze "Dark Ages". PLoS ONE 12(3):1–21.

Smith P. 1982. The physical characteristics and biological affinities of the MB I skeletal remains from Jebel Qa'aqir. Bulletin of the American Schools of Oriental Research.

Stuiver M, Polach HA. 1977. Reporting of C-14 data: discussion. Radiocarbon 19(3):355–363.

Tubb JN. 1990. Excavations at the Early Bronze Age Cemetery of Tiwal esh-Sharqi. London.

Tufnell O. 1958. Lachish IV (Tell ed-Duweir): the Bronze Age. London: Oxford University Press.

Wacker L, Němec M, Bourquin J. 2010. A revolutionary graphitisation system: fully automated, compact and simple. Nuclear Instruments and Methods in Physics Research, Section B: Beam Interactions with Materials and Atoms 268(7–8):931–934.

Weiner S. 2010. Microarchaeology – beyond the visible archaeological record. New York.

Weiner S, Bar-Yosef O. 1990. States of preservation of bones from prehistoric sites in the Near East: a survey. Journal of Archaeological Science 17(2):187–196.

Yan X, Tepper Y, Bar-oz G, Boaretto E. 2021. FTIR bone characterization and radiocarbon dating: timing the abandonment of Byzantine Pigeon Towers in the Negev Desert, Israel. Radiocarbon 63(6):1715–1735.

Yannai E, Nagar Y. 2014. Bet Dagan Intermediate Bronze Age and Mamaluk Period cemeteries. Jerusalem: Israel Antiquities Athority.

Yizhaq M, Mintz G, Cohen I, Khalaily H, Weiner S. 2005. Quality controlled radiocarbon dating of bones and charcoal. Radiocarbon 47(2):193–206.

https://doi.org/10.1017/RDC.2022.58 Published online by Cambridge University Press